

# Diffraction effects in superfluorescence

Yu. A. Avetisyan, A. I. Zaitsev, V. A. Malyshev, and E. D. Trifonov

Leningrad State Pedagogical Institute

(Submitted 9 July 1988)

Zh. Eksp. Teor. Fiz. **95**, 1541–1552 (May 1989)

We study the influence of diffraction effects on characteristics of superfluorescence for a two-dimensional model on the basis of the semiclassical theory. The pulse shape and the directivity diagram are evaluated for superfluorescence in systems with various Fresnel numbers. A stochastic structure, which is due to quantum fluctuations of the initial polarization, is observed in the directivity diagram of the radiation.

## 1. INTRODUCTION

In the majority of theoretical papers devoted to the study of superfluorescence (SF) a one-dimensional model is utilized, in which the dependence of the field and of the characteristics of the medium on the transverse coordinates is ignored.<sup>1–3</sup> However, even in those cases when the geometry of the system picks out a preferred direction for the propagation of the radiation, an account of the divergence and diffraction of the field substantially influences the directivity diagram and kinetics of the process.

The first non one-dimensional quantum models of SF were considered in several papers,<sup>4–8</sup> beginning with Dicke's work.<sup>4</sup> From their results it was possible to estimate the average velocity of radiation in different directions as a function of the geometry of the sample. In later papers<sup>9,10</sup> quantum theory was applied to a detailed description of the initial (linear) stage of SF in three-dimensional systems. In investigating the nonlinear stage of SF the semiclassical approach turns out to be effective.

In Ref. 11 SF was investigated for a two-dimensional model in which the radiators are two parallel infinite threads with dipoles oriented along them. The radiation from such a source (one thread) is isotropic in the two-dimensional space orthogonal to the direction of the thread. The authors discussed the dynamics and directivity diagram of SF of the system of threads with transverse dimension of the order of the wavelength of the light  $\lambda$ .

A more realistic picture of the influence of diffraction effects on the form of the SF pulse is given in Ref. 12. The authors performed calculations for the data corresponding to the experiment of Ref. 13 and showed that taking into account diffraction and fluctuations of the initial polarization improves agreement with experiment.

In Refs. 14–16, the influence of diffraction on the dynamics of superradiation of a planar crystal layer of excited nuclei was investigated.

We investigate here the SF of an extended two-dimensional system, whose length  $L$  and transverse dimension  $D$  satisfy the condition  $L \gg D \gg \lambda$ . Our main interest is in the study of transverse effects and of the directivity diagram of the radiation as a function of the Fresnel number  $F = D^2/\lambda L$  in the range  $0.1 \leq F \leq 10$ . The calculations were performed in the semiclassical approach, assuming a uniform as well as a random initial polarization of the medium. In the latter case fluctuations of the SF pulse parameters (delay times, amplitudes, etc.) were demonstrated in separate realizations. It was shown that the structure of the SF directivity diagram

was also subject to fluctuations from one realization of the pulse to the next.

## 2. STATEMENT OF THE PROBLEM

We shall investigate SF for a two-dimensional model, assuming that the field and atomic characteristics of the system depend on the longitudinal coordinate  $x$  ( $0 \leq x \leq L$ ) and transverse coordinate  $y$  ( $-D/2 \leq y \leq D/2$ ,  $L \gg D$ ). The optical centers will be modeled by a two-level atom with equal frequencies  $\omega_0$  and dipole transition moments  $\mu$ , oriented along the  $z$ -axis.<sup>11</sup> In this model the  $z$ -component of the medium polarization vector  $P_z = P$  is different from zero, as well as three components of the electromagnetic field: one component of the electric vector  $E_z = E$  and two components of the magnetic vector,  $B_x$  and  $B_y$ . The Poynting vector  $S$ , connected with the directivity diagram of the radiation, has in this case the following components:

$$S = \frac{c}{4\pi} [\mathbf{E}\mathbf{B}] = \frac{c}{4\pi} (-EB_y, EB_x, 0). \quad (1)$$

Maxwell's equation for  $P, E, B_x$  and  $B_y$  are written as follows

$$\begin{aligned} \frac{\partial E}{\partial y} &= -\frac{1}{c} \frac{\partial B_x}{\partial t}, & \frac{\partial E}{\partial x} &= \frac{1}{c} \frac{\partial B_y}{\partial t}, \\ \frac{\partial B_y}{\partial x} - \frac{\partial B_x}{\partial y} &= \frac{4\pi}{c} \frac{\partial P}{\partial t} + \frac{1}{c} \frac{\partial E}{\partial t}. \end{aligned} \quad (2)$$

Polarization of the medium is defined as

$$P = N_0 \mu (\rho_{12} + \rho_{21}), \quad (3)$$

where  $N_0$  is the concentration of optical centers and  $\rho_{12} = \rho_{21}^*$  is the off-diagonal element of the atomic density matrix, satisfying the equations

$$\begin{aligned} i\hbar \dot{\rho}_{11} &= \mu E (\rho_{12} - \rho_{21}), \\ i\hbar \dot{\rho}_{22} &= \mu E (\rho_{21} - \rho_{12}), \\ i\hbar \dot{\rho}_{21} &= \hbar \omega_0 \rho_{21} + \mu E (\rho_{22} - \rho_{11}). \end{aligned} \quad (4)$$

Assuming that the fields  $E$  and  $B$  arising in the system are not very large ( $\mu E, \mu B \ll \hbar \omega_0$ ) we isolate in the characteristics of the electromagnetic field and the off-diagonal elements of the density matrix the "fast" dependence, connected with the optical frequency and the radiation wavelength:

$$\rho_{12} = R_1^+ \exp\{i(\omega_0 t - k_0 x)\} + R_2^+ \exp\{i(\omega_0 t + k_0 x)\}, \quad (5a)$$

$$\rho_{21} = R_1^- \exp\{-i(\omega_0 t - k_0 x)\} + R_2^- \exp\{-i(\omega_0 t + k_0 x)\}, \quad (5b)$$

$$\begin{pmatrix} E \\ B_x \\ B_y \end{pmatrix} = \frac{\hbar}{2i\mu\tau_R} \left[ \begin{pmatrix} \epsilon_1^+ \\ b_{1x}^+ \\ b_{1y}^+ \end{pmatrix} \exp\{i(\omega_0 t - k_0 x)\} + \begin{pmatrix} \epsilon_2^+ \\ b_{2x}^+ \\ b_{2y}^+ \end{pmatrix} \exp\{i(\omega_0 t + k_0 x)\} \right] + \text{c.c.} \quad (5c)$$

Here  $k_0 = \omega_0/c$ ,  $\tau_R = \hbar/(4\pi k_0 \mu^2 N_0 L)$  is the SF characteristic time,  $R_j^+ = (R_j^-)^*$ ,  $\epsilon_j^+ = (\epsilon_j^-)^*$ ,  $b_{jx}^+ = (b_{jx}^-)^*$ ,  $b_{jy}^+ = (b_{jy}^-)^*$  are dimensionless polarization amplitudes and components of the electromagnetic field. The index  $j = 1(2)$  describes a wave propagating in the direction of the positive (negative)  $x$  axis. The equations for the slow amplitudes  $R$ ,  $\epsilon$ ,  $b$  (in the longitudinal coordinate and time) are obtained after substitution of (5) into (2) and (4) and neglecting the rapidly oscillating terms

$$\frac{1}{c} \frac{\partial}{\partial t} \begin{pmatrix} \epsilon_1^\pm \\ \epsilon_2^\pm \end{pmatrix} + \frac{\partial}{\partial x} \begin{pmatrix} \epsilon_1^\pm \\ -\epsilon_2^\pm \end{pmatrix} \pm \frac{i}{2k_0} \frac{\partial^2}{\partial y^2} \begin{pmatrix} \epsilon_1^\pm \\ \epsilon_2^\pm \end{pmatrix} = \frac{1}{L} \begin{pmatrix} R_1^\pm \\ R_2^\pm \end{pmatrix}, \quad (6a)$$

$$\frac{\partial}{\partial t} \begin{pmatrix} R_1^\pm \\ R_2^\pm \end{pmatrix} = \frac{1}{\tau_R} Z \begin{pmatrix} \epsilon_1^\pm \\ \epsilon_2^\pm \end{pmatrix}, \quad Z = \frac{1}{2} (\rho_{22} - \rho_{11}), \quad (6b)$$

$$\frac{\partial Z}{\partial t} = -\frac{1}{2\tau_R} (\epsilon_1^+ R_1^- + \epsilon_2^+ R_2^- + \text{c.c.}), \quad (6c)$$

$$b_{jx}^\pm = \pm \frac{i}{k_0} \frac{\partial \epsilon_j^\pm}{\partial y}, \quad b_{jy}^\pm = (-1)^j \epsilon_j^\pm. \quad (6d)$$

We note that we are not making use of the approximation of slow variation of the amplitudes with respect to the transverse coordinate, and the corresponding terms in Eq. (6a) contain second derivatives.

From Eq. (6) follows the local energy conservation law:

$$\frac{\partial}{\partial t} (U_a + U_f) + \text{div } \mathbf{S} = 0, \quad (7)$$

where  $U_a$  and  $U_f$  are the atomic and field energy densities respectively:

$$U_a = N_0 \hbar \omega_0 Z, \quad (8a)$$

$$U_f = \frac{N_0 \hbar \omega_0 L}{2c\tau_R} (|\epsilon_1^\pm|^2 + |\epsilon_2^\pm|^2), \quad (8b)$$

and the vector  $\mathbf{S} = (S_x, S_y, 0)$

$$S_x = \frac{N_0 \hbar \omega_0 L}{2\tau_R} (|\epsilon_1^\pm|^2 - |\epsilon_2^\pm|^2), \quad (9a)$$

$$S_y = \frac{N_0 \hbar \omega_0 L}{2\tau_R} \frac{i}{2k_0} \left( \epsilon_1^- \frac{\partial \epsilon_1^+}{\partial y} - \epsilon_2^+ \frac{\partial \epsilon_2^-}{\partial y} \right) + \text{c.c.} \quad (9b)$$

is the Poynting vector (1), averaged over the field space and time oscillation periods. It is obvious that  $\mathbf{S}$  may be expressed as the difference  $\mathbf{S} = \mathbf{S}_1 - \mathbf{S}_2$ , where the vectors

$$\mathbf{S}_1 = \frac{N_0 \hbar \omega_0 L}{2\tau_R} \left( |\epsilon_1^\pm|^2, \frac{i}{2k_0} \epsilon_1^- \frac{\partial \epsilon_1^+}{\partial y} + \text{c.c.}, 0 \right), \quad (10a)$$

$$\mathbf{S}_2 = \frac{N_0 \hbar \omega_0 L}{2\tau_R} \left( |\epsilon_2^\pm|^2, \frac{i}{2k_0} \epsilon_2^+ \frac{\partial \epsilon_2^-}{\partial y} + \text{c.c.}, 0 \right) \quad (10b)$$

constitute current densities of waves propagating in the di-

rections of the positive and negative  $x$  axis.

It is convenient in solving Eqs. (6) to go over to dimensionless variables  $\tau = t/\tau_R$ ,  $\xi = x/L$ ,  $\eta = y/D$ . In terms of these variables Eqs. (6) become

$$\frac{1}{v} \frac{\partial}{\partial \tau} \begin{pmatrix} \epsilon_1^\pm \\ \epsilon_2^\pm \end{pmatrix} + \frac{\partial}{\partial \xi} \begin{pmatrix} \epsilon_1^\pm \\ -\epsilon_2^\pm \end{pmatrix} \pm \frac{i}{4\pi F} \frac{\partial^2}{\partial \eta^2} \begin{pmatrix} \epsilon_1^\pm \\ \epsilon_2^\pm \end{pmatrix} = \begin{pmatrix} R_1^\pm \\ R_2^\pm \end{pmatrix}, \quad (11a)$$

$$\frac{\partial}{\partial \tau} \begin{pmatrix} R_1^\pm \\ R_2^\pm \end{pmatrix} = Z \begin{pmatrix} \epsilon_1^\pm \\ \epsilon_2^\pm \end{pmatrix}, \quad (11b)$$

$$\frac{\partial Z}{\partial \tau} = -\frac{1}{2} (\epsilon_1^+ R_1^- + \epsilon_2^+ R_2^- + \text{c.c.}). \quad (11c)$$

We have introduced here the dimensionless velocity of light  $v = c\tau_R/L$  and the Fresnel number  $F = D^2/\lambda L$ . We shall also write out the expressions for the dimensionless densities of the energy currents of the opposing waves  $\mathbf{s}_j = (\tau_R/N_0 \hbar \omega_0) (S_{jx}/L, S_{jy}/D, 0)$ :

$$\mathbf{s}_1 = \frac{1}{2} \left( |\epsilon_1^\pm|^2, \frac{i}{4\pi F} \epsilon_1^- \frac{\partial \epsilon_1^+}{\partial \eta} + \text{c.c.}, 0 \right), \quad (12a)$$

$$\mathbf{s}_2 = \frac{1}{2} \left( |\epsilon_2^\pm|^2, \frac{i}{4\pi F} \epsilon_2^+ \frac{\partial \epsilon_2^-}{\partial \eta} + \text{c.c.}, 0 \right). \quad (12b)$$

To solve the system of equations (11) it is necessary to specify the initial and boundary values of the field and atomic variables. Conventionally for the semiclassical SF theory one specifies a vanishing initial field, full inversion, and primary polarization imitating spontaneous emission:

$$\epsilon_j^\pm(\xi, \eta, 0) = 0, \quad (13a)$$

$$Z(\xi, \eta, 0) = 1/2, \quad (13b)$$

$$R_j^\pm(\xi, \eta, 0) = R_{j0}^\pm(\xi, \eta), \quad j=1, 2. \quad (13c)$$

In addition the field should satisfy the boundary conditions

$$\epsilon_1^\pm(0, \eta, \tau) = \epsilon_2^\pm(1, \eta, \tau) = 0, \quad (13d)$$

$$\epsilon_j^\pm(\xi, \eta \rightarrow \pm\infty, \tau) = 0, \quad j=1, 2. \quad (13e)$$

We shall discuss below two ways of specifying the initial polarization: in the form of a constant over the sample value  $R_{j0}^\pm$  and in the form of a Gaussian random function with  $\delta$ -correlation. The first case corresponds to the so-called induced superradiance,<sup>17</sup> when the radiation of the inverted system is initiated by a brief pulse, producing an approximately uniform polarization in the sample, exceeding the level of quantum noise. Specifying the initial polarization in the form of a Gaussian random function is equivalent, as was shown in Ref. 18, to taking into account the quantum fluctuations of the polarization, corresponding to superfluorescence as a spontaneous process.

### 3. SOLUTION OF THE MAXWELL-BLOCH SYSTEM OF EQUATIONS

We confine ourselves to the study of SF for systems with pulse time characteristics corresponding to the one-dimensional model of SF;

$$1/v = L/c\tau_R = 4\pi k_0 \mu^2 N_0 L / \hbar c \ll 1. \quad (14)$$

In that case one may ignore retardation effects, i.e., neglect in the equations for the field (11a) the derivatives with respect to time.

The solution of Eq. (11a), satisfying the boundary conditions (13d) and (13e) and ignoring retardation ( $L/c\tau_R \ll 1$ ), has the form

$$\varepsilon_1^\pm(\xi, \eta, \tau) = \int_0^{\xi} d\xi' \int_{-1/2}^{1/2} d\eta' M^\pm(\xi - \xi', \eta - \eta') R_1^\pm(\xi', \eta', \tau), \quad (15a)$$

$$\varepsilon_2^\pm(\xi, \eta, \tau) = \int_{\xi}^1 d\xi' \int_{-1/2}^{1/2} d\eta' M^\pm(\xi' - \xi, \eta - \eta') R_2^\pm(\xi', \eta', \tau), \quad (15b)$$

where the kernel  $M^\pm$  is given by the formula

$$M^\pm(\xi, \eta) = (\pm iF/\xi)^{1/2} \exp(\mp i\pi F \eta^2/\xi) \quad (16)$$

and describes two-dimensional diffraction of electromagnetic waves.

As a result of the transformation (15) the initial system of partial differential equations (11) reduces to the system of integro-differential equations (11b,c) and (15). This form of Maxwell-Bloch equations is in a number of cases preferable, in particular in the study of statistical properties of SF due to field and polarization quantum fluctuations.

Based on numerical integration of the system of equations (11b,c) and (15), the algorithm and details of which are given in the Appendix, we have evaluated the components of the Poynting vector  $s_x$  and  $s_y$  [see formulas (9)], the full inversion of the atomic system

$$\bar{Z}(\tau) = \int_0^1 d\xi \int_{-1/2}^{1/2} d\eta Z(\xi, \eta, \tau), \quad (17)$$

the radiation intensity referred to one wave

$$I(\tau) = -m^{-1} \partial \bar{Z} / \partial \tau, \quad m=1, 2, \quad (18)$$

and the SF directivity diagram determined by the Umov-Poynting vector in the wave zone ( $\xi \gg 1$ ). Using (15) and (16) we have for this vector

$$\mathbf{S}_j = \mathbf{n} \frac{\hbar \omega_0 N_0 L}{2\tau_R} |\varepsilon_j^\pm|^2 = \mathbf{n} \frac{\hbar \omega_0 N_0 L FL}{2\tau_R} \frac{1}{|x|} |f_j^\pm(\tau, \theta)|^2, \quad (19)$$

where

$$f_j^\pm(\tau, \theta) = \int_0^1 d\xi' \int_{-1/2}^{1/2} d\eta' R_j^\pm(\xi', \eta', \tau) \times \exp\left[\mp i\pi F \frac{L}{D} \theta \left(\frac{L}{D} \theta \xi' - 2\eta'\right)\right]. \quad (20)$$

Here  $j = 1, 2, \mathbf{n}$  is a unit vector directed to the point of observation and lying in the  $x$ - $y$  plane, and  $\theta$  is the angle between  $\mathbf{n}$  and the  $x$  axis. In deriving (19) we used the approximation  $\theta \ll 1$ .

#### 4. UNIFORM INITIAL POLARIZATION

As we have already remarked, specifying uniform initial polarization corresponds to induced superradiance.<sup>17</sup> The calculations were performed for the value  $R_{01}^\pm = 0.02$ . The amplitude of the initial polarization of the second wave  $R_{20}^\pm$  was set equal to zero. In that case that wave does not evolve.

The time dependence of SF intensity obtained for various values of the Fresnel number  $F$  is shown in Fig. 1 (solid curves). A characteristic feature of the SF pulse for  $F \gtrsim 1$  is that between maxima the radiation intensity does not go down to zero, as is true in the one-dimensional theory, but instead goes to some value  $I_{\min}$ . Increasing the Fresnel number  $F$  reduces this value. On the contrary, decreasing  $F$  increases  $I_{\min}$  and at the same time causes the peak intensity of the second maximum to decrease. They become equal for  $F \approx 1/4$ . As a result the oscillatory structure of the SF pulse is smeared out and only one peak is observed in the radiation.

Figures 2–4 show the calculations (in the one-wave approximation) of the distribution of the inversion through the sample (in view of the symmetry of the problem in the coordinate  $\eta$ , we show the distribution over half of the sample only,  $\eta > 0$ ) and the radiation directivity diagrams  $|f_j^\pm(\tau, \theta)|^2$  at various instants of time for values of the Fresnel number  $F = 0.1; 1; 4$ . These figures show a common regularity consisting of early development of inversion in the central part of the sample ( $\eta \approx 0$ ) with relatively late evolution at the edges ( $\eta = 0.5$ ). This is most pronounced for  $F = 1$ . The transverse nonuniformity of the inversion is the reason for the above-mentioned smoothing out of the oscillatory structure of the SF pulse.

With increasing Fresnel number  $F$  the width of the region of synchronous variation of the inversion grows, encompassing an ever larger part of the cross section of the sample. At the same time transverse uniformity is established and the longitudinal directivity of the Poynting vector is strengthened (Fig. 5), ensuring a decrease in the radiation energy flux leaving the sample through its side boundaries.

The divergence of the radiation (Fig. 5) during the major part of the duration of the SF pulse is determined by the angle, equal in order of magnitude to the diffraction angle  $\theta_{\text{dir}} = \lambda/D$ . However, at the instants between the maxima the intensity of the radiation is distributed approximately

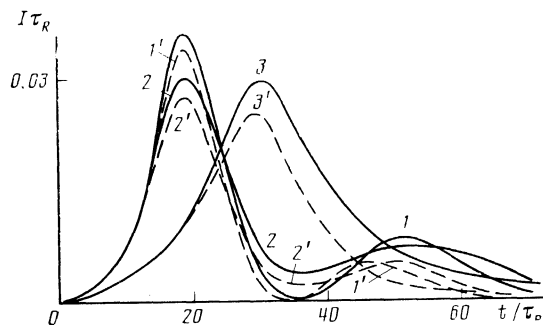


FIG. 1. Intensity of radiation for samples with different Fresnel numbers. Solid curves are for calculations in one-wave approximation, dashed curves—for two-wave. Initial polarization  $R_{01}^\pm = 0.02$ ; 1, 1— $F = \infty$  (one-dimensional solution), 2, 2'— $F = 1$ , 3, 3'— $F = 0.1$ .

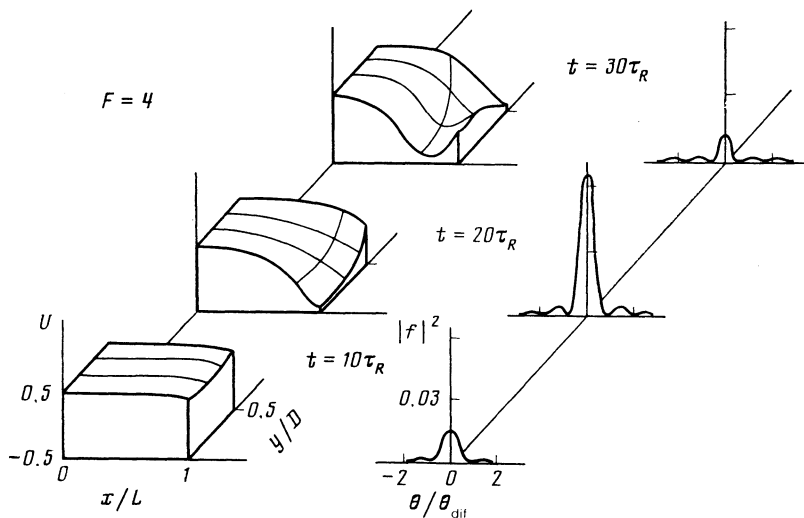


FIG. 2. Inversion distribution in the sample (left) and radiation directivity diagram (right) at different instants of time for Fresnel number  $F = 4$ . Initial polarization uniform throughout the sample.

equally over the diffraction side lobes located within the limits of the geometrical angle  $\theta_{\text{geom}} = D/L$ , and decreases in size with increasing  $F$ .

In this manner, for uniform initial polarization, increasing the Fresnel number causes in the SF pulse to approach in its properties the pulse corresponding to the one-dimensional model of SF.

For small Fresnel numbers, with increasing distance from the axis of the sample the transverse component of the Poynting vector increases rapidly (Fig. 5), which indicates that an increasing fraction of the energy leaves the sample through its side boundaries. Thus, the ratio of the sum of the side radiation energy fluxes to the longitudinal at the maximum instant of the SF pulse equals approximately  $3/2$  for  $F = 0.1$ , while this ratio is close to  $0.1$  for  $F = 1$ . The intense radiation in the transverse directions determines the distinctive property of the SF pulse for  $F \ll 1$ : establishment of transverse uniformity of atom-field characteristics, increase in the delay time, decrease in the peak value of the intensity, and increase in the width of the SF pulse.

The directivity diagram of the radiation in the case of small Fresnel numbers (Fig. 4) testifies to the divergence of SF within the limits of the diffraction angle  $\theta_{\text{dif}} = \lambda/D$ .

The results described above were obtained in the one-wave approximation. To illustrate the effect of the second wave on the SF characteristics we show in Fig. 1 the results of the calculation of the SF intensity (dashed curves) when the symmetric opposing wave ( $R_{20}^{\pm} = 0.02$ ) is taken into account. According to Fig. 1 taking into account the opposing wave affects mainly the later stages of evolution of SF, resulting in the case of  $F \gtrsim 1$  in a suppression of the intensity oscillations. With decreasing Fresnel number ( $F < 1$ ) the role of the opposing wave increases and manifests itself in a decrease of the delay time and of the maximum value of the SF intensity, as compared to the one-wave approximation.

We also note that calculations performed for small Fresnel numbers with the opposing wave taken into account, whose results are not shown in Figs. 2–5, showed a tendency towards establishing spatial uniformity of atom-field characteristics not only in the transverse but also in the longitudinal direction. This circumstance justifies the formulas, proposed in Ref. 19, for the description of SF kinetics for  $F \ll 1$ :

$$\bar{Z}(\tau) = -\frac{1}{2} \text{th}[\alpha(\tau - \tau_D)/2], \quad (21a)$$

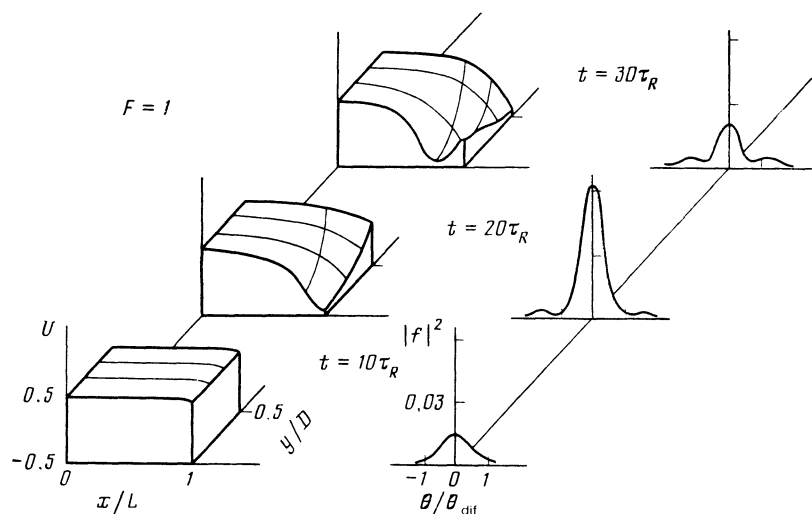


FIG. 3. Same as Fig. 2, for  $F = 1$ .

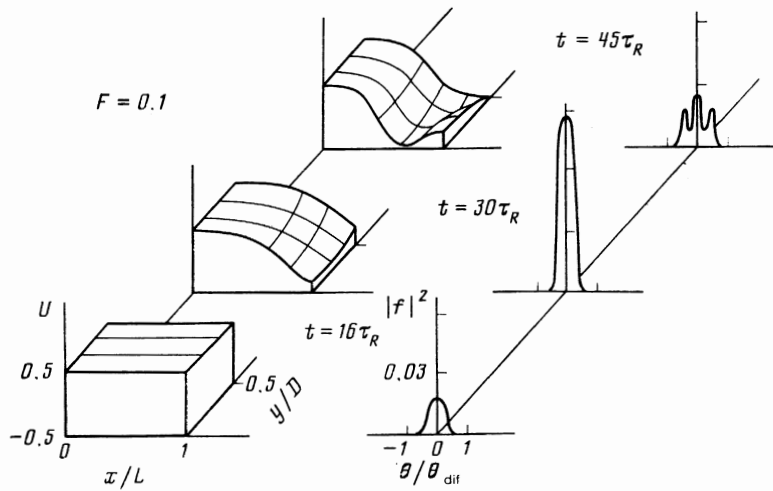


FIG. 4. Same as Fig. 2, for  $F = 0.1$ .

$$I(\tau) = \frac{\alpha}{4} \operatorname{sech}^2[\alpha(\tau - \tau_D)/2], \quad (21b)$$

$$\alpha = \frac{4}{3} \left(\frac{F}{2}\right)^{1/2}, \quad \tau_D = \frac{2}{\alpha} \ln \frac{1}{2^{1/2} |R_0^\pm|} \quad (21c)$$

### 5. RANDOM INITIAL POLARIZATION

Superfluorescence as a spontaneous process is due to quantum fluctuations of the field, which can be consistently described using quantum electrodynamics. However, it was shown by the authors of Ref. 18 that the quantum fluctuations of the field can be effectively taken into account in the semiclassical approach if the amplitude of initial polarization  $R_0^\pm(\xi, \eta)$  is taken to be a Gaussian complex random function with  $\delta$ -correlation.

We have performed a number of calculations of the emission kinetics and the radiation directivity diagram using

the one-wave approximation for a specified constant modulus of the initial polarization  $|R_{10}^\pm| = 0.1$  and random values of its phase in the interval  $[0, 2\pi]$ .

SF pulses evaluated for three random realizations of the initial polarization are shown in Fig. 6. As can be seen, fluctuations in the polarization appear in the fluctuations of the parameters of the SF pulse: its form, delay time and peak intensity. The largest fluctuations are experienced by the parameters of the SF pulse for systems with small Fresnel number, while for  $F = 1$  the fluctuations are smallest. With increasing Fresnel number the effect of the fluctuations of the initial polarization on the delay time is weakened, but the scatter in the peak values of SF intensity remains, as before, significant.

Figure 7 demonstrates the evolution in time of the SF directivity diagram for a typical realization of the distribution of the initial polarization. The ray structure of the SF directivity diagram is particularly clear, as well as the competition between rays propagating at different angles to the axis of the sample. These angles undergo strong fluctuations

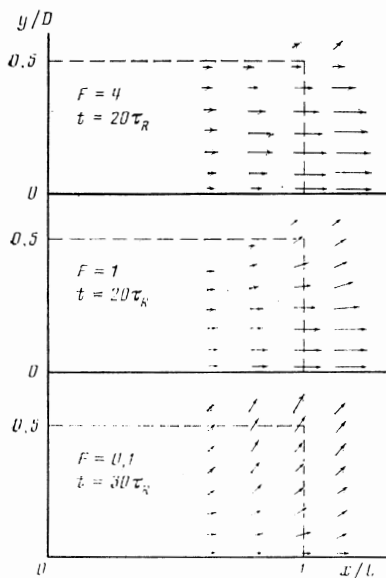


FIG. 5. The Poynting vector field for maximal intensity of radiation. Initial polarization uniform throughout the sample,  $a = 0.56$ ,  $b = 1.125$ .

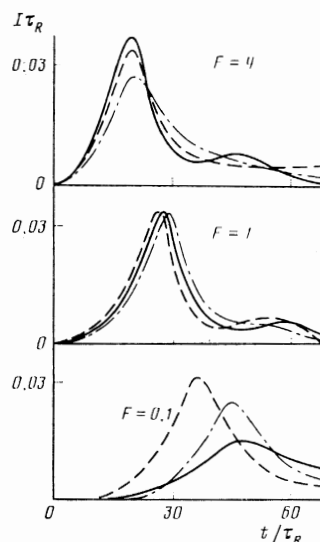


FIG. 6. Emission pulses for various random realizations of initial polarization and Fresnel numbers  $F$ .

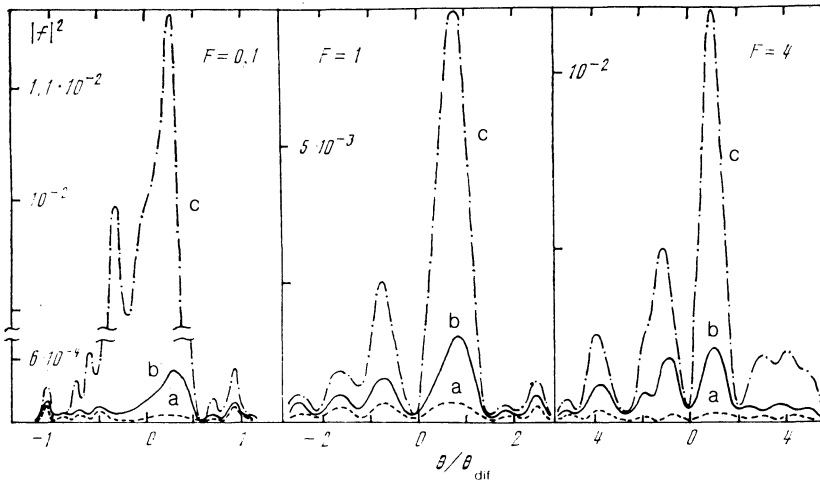


FIG. 7. Structure of the directivity diagram for random realization of initial polarization at different instants of time for  $F=0.1$ : a— $t=\tau_R$ , b— $10\tau_R$ , c— $30\tau_R$ ; for  $F=1$  and  $F=4$ : a— $t=\tau_R$ , b— $5\tau_R$ , c— $10\tau_R$ .

from one realization to the next. For large Fresnel numbers ( $F > 1$ ) the indicated fluctuations lie within the limits of the angular dimension  $D/L$  of the sample, with the angular dimension of an individual ray having the diffraction scale  $\lambda/D$ . In this manner the number of the rays equals approximately the Fresnel number:  $(D/L)/(\lambda/D) = D^2/\lambda L = F$ . For small Fresnel numbers ( $F < 1$ ) the total width of the directivity diagram is determined by the diffraction angle, and the angular dimensions of the system are manifested in the structure.

## 6. CONCLUSION

We have described SF taking into account diffraction effects as well as quantum fluctuations of the initial polarization.

For systems with Fresnel number  $F \gg 1$  the time scale of the pulse turns out to be the same as in the one-dimensional model. However, quantum fluctuations of the initial polarization give rise to transverse nonuniformity of atomic and field characteristics, which manifests itself in a change in the shape of the pulse and in the radiation directivity diagram. The pulse shape becomes smoother, the oscillations characteristic of the one-dimensional model become smoothed out. The SF directivity diagram has a ray structure with angular dimensions of individual components (rays) of the order of the diffraction angle  $\lambda/D$ . Since the full width of the directivity diagram is of the order of the geometric angle  $D/L$ , the number of rays (for the two-dimensional model) approximately equals the Fresnel number  $F$ . Due to the competition between the rays, some of them evolve earlier, with a stochastic intensity distribution as the result.

With decreasing Fresnel number ( $F < 1$ ) the time scale increases as  $\sim F^{-1/2}$ , and the spatial dependence of the inversion and the slow amplitudes of the field and polarization smooths out. This results in a SF pulse shape with one maximum and a practically one-ray character of the directivity diagram. The angular dimension of the ray equals the diffraction angle  $\lambda/D$ , and its form changes relatively little in going from one realization of the distribution of the initial polarization to another.

In Ref. 20 diffraction of superfluorescence was observed in the  $KCl:O_2^-$  crystal. In these experiments the excitation region was created with the help of a cylindrical lens and constituted a planar layer, whose width was determined

by the absorption depth in accordance with Beer's law. With increased pumping intensity the number of diffraction maxima increased from 1 to 4. Although this problem is in essence two-dimensional, quantitative comparison with experiment requires calculations using [instead of (16)] the Green function for the three-dimensional wave equation.

In conclusion the authors thank V. I. Perel' for discussion of the results.

## APPENDIX

The integration region  $G$  was taken somewhat larger than the size of the system, to permit determination of the field inside as well as outside the sample. In the plane of the dimensionless coordinates  $(\xi, \eta)$ ,  $G$  was chosen as a rectangle with sides  $2a \gg 1$  and  $b \gg 1$ . The region was divided by a uniform grid into rectangular subregions (cells) of dimension  $H_\xi \times H_\eta$ , numbered by the indices and  $k, l$  (Fig. 8). It was assumed in the calculation scheme that the inversion and polarization had a constant value inside a fixed cell  $(k, l)$ , with the field  $\varepsilon_{ki}$  equal to the sum of the contributions of the fields from cells to the left of the fixed cell  $(k, l)$  and acting at its center with coordinates  $\xi_k = (k + \frac{1}{2})H_\xi$ ,  $\eta_l = lH_\eta$ :

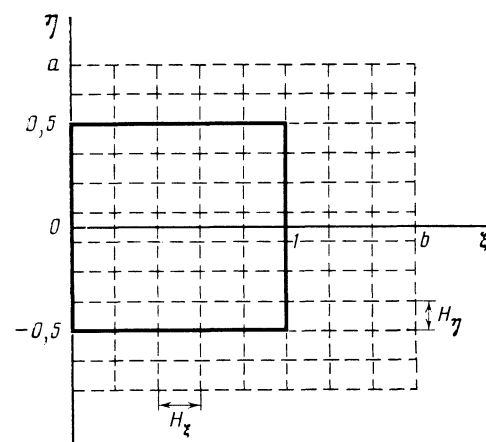


FIG. 8. The grid scheme for numerical integration of the Maxwell-Bloch system of equations. The solid line denotes the contour of the sample.

$$\epsilon_{kl}^{\pm} = \sum_{k' \leq k} \sum_{l'} \bar{M}_{k-k', l-l'}^{\pm} R_{k'l'}^{\pm}, \quad (\text{A1})$$

$$\bar{M}_{k-k', l-l'}^{\pm} = \int_{k'H_{\xi}}^{(k'+1)H_{\xi}} d\xi' \int_{(l'-1/2)H_{\eta}}^{(l'+1/2)H_{\eta}} d\eta' \left( \pm i \frac{F}{\xi_k - \xi'} \right)^{1/2} \times \exp \left[ \mp i\pi F \frac{(\eta_l - \eta')^2}{\xi_k - \xi'} \right] \theta(\xi_k - \xi'). \quad (\text{A2})$$

The Heavyside function  $\theta(x)$  in Eq. (A2) is introduced to take correctly into account the contribution of the polarizations of the cells  $(k', l')$  to the field acting on the cell  $(k, l)$ .

The expression for the kernel  $M^{\pm}$  may be transformed into

$$\bar{M}_{kl}^{\pm} = \bar{M}_{k,-l}^{\pm} = Q^{\pm}(\xi_k, \eta_l + H_{\eta}/2) - Q^{\pm}(\xi_k, \eta_l - H_{\eta}/2) + Q^{\pm}(\xi_{k-1}, \eta_l - H_{\eta}/2) - Q^{\pm}(\xi_{k-1}, \eta_l + H_{\eta}/2), \quad (\text{A3})$$

$$Q^{\pm} = (\pm i)^{1/2} \xi [ (1 \pm 2\pi i u^2) \Phi^{\pm}(u) + u \exp(\mp i\pi u^2) ], \quad (\text{A4})$$

where  $u = (F/\xi)^{1/2} \eta$  and  $\Phi^{\pm}(u)$  are the Fresnel integrals

$$\Phi^{\pm}(u) = \int_0^u dt \exp(\mp i\pi t^2). \quad (\text{A5})$$

For  $k = 0$  the last two terms in formula (A3) are understood as the limiting values of the corresponding expressions (for  $\xi_{-1} \rightarrow +0$ ), which remain finite for arbitrary values of the index  $l$  and for  $l = 0$  correspond to the contribution due to the polarization of the given cell to the field calculated for it, i.e. "self-action."

The requirement of smooth variation of the kernel  $M_{kl}^{\pm}$  in going from one cell to the next, necessary for correct replacement of the integral relation (15) by the algebraic (A1), imposes definite restrictions on the number of grid points  $N_{\xi} = 1/H_{\xi}$ ,  $N_{\eta} = 1/H_{\eta}$ , corresponding to the size of the integration region. For large values of the Fresnel number the indicated smoothness is ensured for  $N_{\xi}, N_{\eta} \gg 1$ . For small values of  $F$ —for  $N_{\xi} \gg 1/F$ ,  $N_{\eta} \gg 1$ .

In this manner the initial system of partial differential equations (11) was reduced to a system of ordinary differen-

tial equations (in time) (11b,c) and (A1), which was solved by standard methods.

In specifying the uniform initial polarization the integration region was broken up into 300 cells in a scheme  $12 \times 25$  ( $H_{\xi} = 1/12, H_{\eta} = 1/25$ ). In calculations with random initial polarization we used instead  $10 \times 15 = 150$  cells ( $H_{\xi} = 0.1, H_{\eta} = 1/15$ ).

The quality control of the numerical solution of the Maxwell-Bloch system of equations was achieved by testing the conservation laws for the energy (7) and for the length of the Bloch vector  $|R_1^{\pm}|^2 + |R_2^{\pm}|^2 + Z^2 = \text{const}$ .

The method employed by us to integrate the Maxwell-Bloch equations can be extended to three-dimensional systems, as well as to the case of scattered orientations of atomic dipoles. The latter is of interest in the study of the polarizing properties of superfluorescence.

<sup>1)</sup> The two-dimensional model may be applied to systems with pronounced anisotropy of optical properties. It allows the determination of the directivity diagram in the plane perpendicular to the axis of anisotropy. An example of such a system can be a uniaxial crystal.

<sup>1</sup> A. V. Andreev, V. I. Emelyanov, and Yu. A. Il'inskiĭ, Usp. Fiz. Nauk **131**, 653 (1980) [Sov. Phys. Usp. **23**, 493 (1980)]. *Kooperativnye yavleniya v optike* [in Russian], Nauka, 1988.

<sup>2</sup> *Theory of cooperative coherent effects in radiation*, [in Russian], Edited by E. D. Trifonov, Leningrad, Leningrad Univ. Press, 1980.

<sup>3</sup> M. Gross and S. Haroche, Phys. Rep. **93**, 301 (1982).

<sup>4</sup> R. H. Dicke, Phys. Rev. **93**, 99 (1954).

<sup>5</sup> N. E. Rehler and J. H. Eberly, Phys. Rev. A **3**, 1735 (1971).

<sup>6</sup> I. V. Sokolov and E. D. Trifonov, Zh. Eksp. Teor. Fiz. **67**, 481 (1974) [Sov. Phys. JETP **40**, 238 (1974)].

<sup>7</sup> E. Ressayre and A. Tallet, Phys. Rev. Lett. **37**, 424 (1976).

<sup>8</sup> R. Bonifacio and L. A. Lugiato, Phys. Rev. A **11**, 1507 (1975); **A12**, 587 (1975).

<sup>9</sup> J. Mostowski and B. Sobolewska, Phys. Rev. A **28**, 2573, 2943 (1983); **A34**, 3109 (1986).

<sup>10</sup> R. J. Glauber and S. Prasad, Phys. Rev. A **31**, 1583 (1985).

<sup>11</sup> A. V. Karnyukhin, R. N. Kuz'min, and V. A. Namiot, Zh. Eksp. Teor. Fiz. **84**, 878 (1983) [Sov. Phys. JETP **57**, 509 (1983)].

<sup>12</sup> E. A. Watson *et al.*, Phys. Rev. A **27**, 1427 (1983).

<sup>13</sup> Q. M. F. Vrehen and J. J. der Weduwe, Phys. Rev. A **24**, 2857 (1981).

<sup>14</sup> A. V. Andreev, O. Yu. Tikhomirov, and M. O. Shaĭymkulov, Izv. AN SSSR ser. fiz. **50**, 1507 (1986).

<sup>15</sup> A. V. Andreev, O. Yu. Tikhomirov, and M. O. Shaĭymkulov, DAN SSSR **296**, 77 (1987) [Sov. Phys. Dokl. **32**, 712 (1987)].

<sup>16</sup> A. V. Andreev, O. Yu. Tikhomirov, and M. O. Shaĭymkulov, Zh. Tekh. Fiz. **57**, 1782 (1987) [Sov. Phys. Tech. Phys. **32**, 1066 (1987)].

<sup>17</sup> R. F. Malikov and E. D. Trifonov, Opt. Commun. **52**, 74 (1984).

<sup>18</sup> F. Haake *et al.* Phys. Rev. A **20**, 2047 (1979).

<sup>19</sup> Yu. A. Avetisyan, in: *Cooperative radiation and photon statistics* [in Russian], E. D. Trifonov, ed., Univ. Press, Leningrad; 1986, p. 56.

<sup>20</sup> A. Schiller, L. O. Schwan, and H. D. Schmid, J. Lumin. **38**, 243 (1987); **40/41**, 541 (1988).

Translated by Adam M. Bincer